HIGH VIRULENCE SELECTS FOR FAST HOST RESISTANCE EVOLUTION

CAROLIN C. WENDLING[1,2*]
JANINA LANGE[1]
HEIKO LIESEGANG[3]
ANJA PÖHLEIN[3]
BOYKE BUNG[4]
JELENA RAIKOV[1]
HENRY GÖHLICH[1]
OLIVIA ROTH[1]
MICHAEL A. BROCKHURST[5]

Addresses:

[1]GEOMAR Helmholtz Centre for Ocean Research Kiel, Marine Evolutionary Ecology, Düsternbrooker Weg 20, 24105 Kiel, Germany

[2]ETH Zürich, Institute of Integrative Biology, Universitätstrasse 16, CHN D 33, 8092 Zürich, Switzerland

[3]Georg-August-University Göttingen, department of genomic and applied microbiology, Grisebachstr 8 37077 Göttingen, Germany.

[4]Leibniz Institute DSMZ-German Collection of Microorganisms and Cell Cultures, Department Bioinformatics and Databases, Inhoffenstr. 7B, 38114 Braunschweig, Germany

[5]Division of Evolution and Genomic Sciences, University of Manchester, Dover Street, Manchester M13 9PT, UK

*Corresponding author:
E-mail: carolin.wendling@env.ethz.ch; Phone: +41 44 633 80 26

ABSTRACT

Infectious organisms can vary tremendously in their virulence. While the evolution of virulence and different levels thereof has received much attention over the past decades, the evolution of host resistance in response to different levels of virulence is far less understood. We expect benefits of host resistance relative to the costs of disease symptoms to be higher against highly virulent compared to low virulent infections and hypothesised that high virulence will select for faster resistance evolution, and ultimately shorter epidemics if parasites fail to overcome these evolved host resistances. To test this hypothesis, we performed a bacteria-phage co-evolution experiment using two filamentous phages that differ in their virulence. We found that resistance to filamentous phages can emerge via two ways: (1) superinfection exclusion, whereby the phage becomes part of the bacterial genome and protects its host against subsequent phage infections, and (2) surface-receptor modifications which prevent phages from entering the host cell. While superinfection exclusion emerged at a similar rate against both phages we observed that resistance evolution through surface-receptor modifications emerged significantly faster against the high virulent phage. This resulted in faster phage extinction and suggests that we can expect shorter epidemics in highly virulent infections, when viruses are unable to overcome host resistance evolution.

Keywords: filamentous phages, experimental evolution, virus, virulence

INTRODUCTION

Infectious agents vary strikingly in virulence and the resulting selection they impose on their host. While some human viruses such as Ebola or rabies can cause a deadly disease, others (including many cold viruses) often remain asymptomatic. Even closely related viruses, such as different strains of myxoma (Fenner and Marshall 1957), or corona viruses (Weiss and Leibowitz 2011) can differ tremendously in virulence. The evolution of different levels of virulence has been suggested to result from a trade-off between parasite reproduction and transmission (Anderson and May 1982, May and Anderson 1983). Higher reproduction results in higher virulence but also in higher host morbidity and mortality and thus limited chances for transmission. Accordingly, virulence increases with natural selection, but only until the threshold where the costs of transmission, caused by the harm to the host, are outweighed by the transmission benefits.

The evolution of virulence has been studied extensively during the last two decades, both using selection experiments (Bull, Molineux et al. 1991, Turner, Cooper et al. 1998, Messenger, Molineux et al. 1999) and parasites evolved in nature (Herre 1993, Ebert 1994). What remains open, however, is the question of how virulence will impact evolutionary trajectories of resistance in a host population, and how these trajectories change with different levels of virulence. Severe disease symptoms resulting from highly virulent infections will significantly reduce host fitness imposing a strong need for hosts to quickly acquire resistance, for instance through evolutionary changes. Thus, we expect benefits of host resistance relative to the costs of disease symptoms to be higher against highly virulent compared to low virulent infections. If this holds true, high virulence will lead to a stronger and thus faster selection for host resistance, and ultimately shorter epidemics if parasites fail to overcome these evolved host resistances.

To explore how variation in virulence between closely related viruses influences the dynamics of host resistance evolution, we designed a co-evolution experiment using the model strain *Vibrio alginolyticus* K01M1 as a host and two closely related versions of the filamentous *Vibrio* phage VALGΦ8, that differ in their replication rate and hence in their virulence (Table 1)(Chibani, Hertel et al. 2020). Filamentous phages (family *Inoviridae*), i.e., long, thin proteinaceous filaments which contain a circular single-stranded DNA genome have been shown to be ideal model systems to study virulence evolution (Bull, Molineux et al. 1991, Messenger, Molineux et al. 1999). These phages can establish chronic infections whereby virions are continuously released without lysis. Even though filamentous phages do not kill their host, they can inflict harm on them as infections typically lead to reduced growth rates. This is because the host cell pays the metabolic costs resulting from phage replication and through phage-encoded proteins inserted into the bacterial membrane (Mai-Prochnow, Hui et al. 2015). Thus, the virulence of filamentous phages, which can vary tremendously across phage types (Rakonjac 2012), can be directly quantified by measuring the reduction in bacterial growth rate.

By combining experimental evolution and whole genome sequencing, we show that resistance by super-infection exclusion (i.e., infected bacteria became resistant to further infection) is a fast way to acquire phage resistance and occurs at a similar rate in both treatments. In contrast, selection for resistance evolution, i.e., surface receptor modifications, is significantly stronger against high virulent compared to low virulent phages. This resulted in faster phage extinction and ultimately shorter epidemics in bacterial lineages that rapidly evolved resistance against high virulent infections.

MATERIAL AND METHODS

(a) Strains and culture conditions

Experiments were conducted using the *Vibrio alginolyticus* strain K01M1 (Chibani, Roth et al. 2020). K01M1 contains one integrated filamentous *Vibrio* phage VALGΦ6 (later called: resident K01M1Φ-phage throughout the manuscript), which replicates at a very low frequency (Chibani, Hertel et al. 2020). Compared to other, closely related *V. alginolyticus* strains, K01M1 is highly susceptible to infections by filamentous phages (Wendling, Piecyk et al. 2017). For the selection experiment we used two different versions of the filamentous *Vibrio* phage VALGΦ8 (Table 1), one integrative (isolated from the host strain K04M5) and one episomal (isolated from the host strain K04M1). While both phages have been shown to significantly reduce the growth of K01M1 (Wendling, Piecyk et al. 2017, Wendling, Goehlich et al. 2018), infections with the high virulent phage impose a significantly stronger reduction in bacterial growth than infections with the low virulent phage. All experiments were carried out in liquid medium (Medium101: 0.5% (w/v) peptone, 0.3% (w/v) meat extract, 3.0% (w/v) NaCl in MilliQ water) at 25° C in 30-ml microcosms containing 6 ml of medium with constant shaking at 180 rpm.

Table 1 Bacteria and phages (including NCBI accession numbers) used in the present study.

Isolate	Accession Number(s)	Phages	Role in evolution experiment
V. alginolyticus K01M1	CP017889.1 CP017890.1	*Vibrio* phage VALGΦ6	Host strain during evolution experiment
V. alginolyticus K04M1	CP017891.1 CP017892.1	*Vibrio* phage VALGΦ6 *Vibrio* phage VALGΦ8 (episomal)	Donor of the episomal, low virulent phage
V. alginolyticus K04M5	CP017899.1 CP017900.1	*Vibrio* phage VALGΦ6 *Vibrio* phage VALGΦ8 (integrative on CR2)	Donor of the integrative, hig virulent phage
Vibrio phage VALGΦ6	MN690600		Resident phage in ancestral K01M1
Vibrio phage VALGΦ8	MN719123		Co-evolving phage in evolution experiment

125 (b) Selection experiment

126 Six replicate populations were founded for each of three treatments from
127 independent clones of K01M1. Treatments comprised (a) a high virulent, integrative
128 version of the filamentous *Vibrio* phage VALGΦ8, later called VALGΦ8$_{K04M1}$, (b) a
129 low virulent, episomal version of the filamentous *Vibrio* phage VALGΦ8, later called
130 VALGΦ8$_{K04M5,}$ and (c) no phage as control. Each population was established from 60 µl
131 of an independent overnight culture (5×10^{8} CFU/ml). At the beginning of the
132 experiment, we inoculated phage-containing treatments with 300 µl of a 5×10^{10} PFU/ml
133 stock solution. Populations were propagated by transferring 1% to fresh medium every
134 24 hours for a total of 30 transfers. On transfer T0, T1, T2 followed by every other
135 transfer, phage and bacterial densities were determined, as described below and whole
136 population samples were frozen at -80° C at a final concentration of 33% glycerol. In
137 addition, on transfer T0, T1, T2, T6, followed by every sixth transfer 24 single colonies
138 were isolated at random from each population and stored at -80° C. Two populations
139 from the control treatment tested positive for virus infection, indicating contamination,
140 were excluded from later assays.
141
142 (c) Bacterial and phage densities

143 *Bacterial densities*: bacterial densities were determined by plating out 100 µl of a
144 dilution series ranging from 10^{-5} to 10^{-7} on *Vibrio* selective Thiosulfate Citrate Bile
145 Sucrose Agar (TCBS) plates (Fluka Analytica). Plates were incubated over night at 25°
146 C and the total amount of colonies was counted the following day.

147 *Phage densities*: Quantification of filamentous phages by standard spot assays is
148 often not possible (Rakonjac 2011). Instead of typical lytic plaques we mostly observed
149 opaque zonas of reduced growth. Thus, we used spectrometry to quantify phage

prevalence (http://www.abdesignlabs.com/technical-resources/bacteriophage-spectrophotometry), which uses the constant relationship between the length of viral DNA and the amount of the major coat protein VIII of filamentous phages, which, together, are the main contributors of the absorption spectrum in the UV range. The amount of phage particles per ml can be calculated according to the following formula:

$$phages/ml = \frac{(OD269 - OD320) * 6e16}{bp},$$

where OD269 and OD320 stand for optical density at 269 and 320 nm and bp stands for number of base pairs per phage.

This method is based on small-scale precipitation of phages by single PEG-precipitation. After centrifuging 1500 µl of the phage containing overnight culture at 13,000 ×g for 2 min, 1200 µl of the supernatant was mixed with 300 µl PEG/NaCl 5× and incubated on ice for 30 min. Afterwards phage particles were pelleted by two rounds of centrifugation at 13,000 ×g for 2 min, resuspended in 120 µl TBS 1× and incubated on ice. After one hour the suspension was cleaned by centrifugation at 13,000 ×g for 1 min and absorbance was measured at 269 and 320 nm.

Quantification of filamentous phages using spectrometry is likely to be erroneous if viral load is low. Therefore, we additionally quantified phage prevalence/ phage extinction in each of the populations on every second transfer day by standard spot assays with a serial dilution (10^{-1} to 10^{-6}) on the ancestral host (for details see (Wendling, Piecyk et al. 2017)) and measured until which dilution the typical opaque zones of reduced bacterial growth were visible.

(d) Measuring phage-resistance

We measured the rate of phage resistance evolution among bacteria against the ancestral phage by determining the reduction in bacterial growth rate (RBG) imposed by

the phage, adapted from (Poullain, Gandon et al. 2008) with some modifications according to (Goehlich, Roth et al. 2019). Twenty-four random colonies from each population from transfer T0, T1, T2, T6, T12, T18, T24, and T30 were introduced into 96-well microtiter plates containing Medium101 at a concentration of 5×10^6 cells/ml and inoculated with ~2.5×10^6 PFU/ml of each of the two ancestral phages used for the selection experiment or without phage (control). Absorbance at 600 nm was measured using an automated plate reader (TECAN infinite M200) at T0 and again after 20 hours of static incubation at 25°C. The reduction in bacterial absorbance 'RBG' was calculated according to the following formula:

$$RBG = \frac{OD600(t=20) - OD600(t=0)[Phage]}{OD600(t=20) - OD600(t=0)[Control]},$$

where OD stands for optical density at 600nm.

(e) Frequency of prophage carriage

On transfer T0, T1, T2, T6 followed by every sixth transfer we measured the frequency of phage carriage of 24 random clones per population using standard PCR. Primers (VALGΦ8_Forward TGGAAGTGCCAAGGTTTGGT, VALGΦ8_Revers GAAGACCAGGTGGCGGTAAA) that specifically target the co-evolving *Vibrio* phage VALGΦ8 have been designed using NCBI Primer-BLAST webpage (httdol://www.ncbi.nlm.nih.gov/tools/primer-blast/). Note, while this primer-pair detects the presence/ absence of *Vibrio* phage VALGΦ8, it does not confirm chromosomal integration of the respective phage. Glycerol stocks were inoculated overnight (25°C, 180 rpm) in Medium 101 and subsequently diluted (1:10) in HPLC purified H_2O and frozen at -80° C. One µl of this suspension was used as DNA template in the PCR assay. Reaction comprised 1 µl Dream Tag Buffer, 0.1 µl Dream Tag DNA polymerase (Thermo Scientific, USA), 4.9 µl H_2O, 1 µl dNTPs [5 mM] and 1 µl of each primer [50

µM]. The amplification program used consisted of: (i) 3 min at 95° C, (ii) 35 cycles of 45 sec at 95° C, 30 sec at 63° C, 45 sec at 72° C, (iii) 7 min at 72° C. Afterwards, 5 µl of each reaction was mixed with 2 µl loading dye (10×) and loaded onto a 1.2% agarose gel dissolved in 1×TAE gel buffer. GeneRuler Express DNA-ladder was used as size marker. Agarose gels were run 15 min at 70 V in 0.5× TAE running buffer and subsequently stained with ethidium bromide for 10 min. DNA was visualized using UV light and documentation took place using Intas Gel iX20 Imager. Phage presence was recorded positive if a PCR product of 1400 bp was visible.

For all subsequent assays, we randomly picked one phage-resistant clone with a positive PCR product (later called: Φ-carrier) and one phage-resistant clone with a negative PCR product (later called: mutant) from each phage-evolved population as well as two randomly selected non-resistant clones from the control populations.

(f) Competition experiments

To determine differences in fitness between both resistance forms, we measured the competitive fitness of Φ-carrier relative to mutants. Each competition culture was done in triplicates as described in (Harrison, Guymer et al. 2015). In brief, overnight cultures of both competing strains (of which one was labelled with a GFP-marker) were mixed 1:1 and 60 µl of this mixture was inoculated to 6 ml Medium 101 to initiate each competitive culture. After 24 hours, fitness was estimated by means of flow cytometry (FACS-Caliburm Becton & Dickinson, Heidelberg, GER), where absolute fluorescent cells and non-fluorescent cells were calculated. Competitive fitness was estimated as the ratio in Malthusian parameters (Lenski, Rose et al. 1991):

$$W = \ln(abundance_{t=24}/abundance_{t=0})_{competitor1} / \ln(abundance_{t=24}/abundance_{t=0})_{competitor2}$$

(g) Bacterial growth rate and phage production

To determine fitness parameters that could explain observed differences in competitive fitness we additionally quantified bacterial growth rate (μ) by means of 24-hour growth curves and phage production using PEG precipitation (as described in (c)) of the same clones used for the competition assays (i.e., one Φ-carrier and one mutant from each phage-treated population and two random phage-susceptible clones from the control populations plus the ancestor).

(h) Whole genome sequencing

We used a combination of long- and short read sequencing to obtain complete genomes of the same clones from the assays above, i.e., one Φ-carrier and one mutant from each phage-treated population and one random phage-susceptible clone from each control population, which corresponds to six independently evolved clones per treatment and resistance form. High molecular weight DNA was extracted from cell pellets of overnight cultures following the protocol for gram negative bacteria from the DNeasy Blood & Tissue Kit (Qiagen, Hilden, Germany). For long-read sequencing the library was prepared using Pacific Bioscience protocol for SMRTbell™ Libraries using PacBio® Barcoded Adapters for Multiplex SMRT® Sequencing. To do so, DNA was fragmented into 10kb fragments using g-tubes (Covaris). Samples were pooled during library preparation aiming for equimolar pooling and library size was selected using Ampure beads. The library was sequenced on a PacBio Sequel instrument using Sequel Polymerase v3.9, SMRT cells v3 LR and Sequencing chemistry v3.0. Loading was performed by diffusion. Two SMRT cells were sequenced (movie time: 600min, pre-extension time: 240 min). Reads were demultiplexed using Barcoding pipeline on

SMRT Link (v6.0.0.47841, SMRT Link Analysis Services and GUI v6.0.0.47836) with 40 as a minimum barcode score.

Short-read sequencing was done on an Illumina 2500 platform and resulted in a minimum average coverage of 88× per strain (coverage range was from 88× to 157×). The reads were quality controlled using the program FastQC Version 0.11.5. High quality reads were used for hybrid assemblies as well as for single nucleotide variation analysis.

Genome assemblies were performed in two different ways: In a first approach assemblies were performed using the Unicycler pipeline (v0.4.7) and the programs within. Assemblies were performed as hybrid assemblies using short-read and long read data in a short-read first approach. In brief: An initial assembly was performed with short-read only using spades (v3.13.0) as provided within Unicycler. The resulting contigs were co-assembled with long-read data using miniasm (v0.2-r168) and curated using the racoon software. This step resulted in complete closed replicons. All long reads were mapped and integrated into the contigs. All replicons were polished using the Pilon software (1.22) to clear any small-scale assembly errors. Finally, all replicons were rearranged according to the origin of replication. The assembly for the ancestral K01M1 strain, as has been described in (Wendling, Piecyk et al. 2017) was performed following the Hierarchical Genome Assembly Process (HGAP3) protocol, developed for Pacific Biosciences Single Molecule Real-Time (SMRT) sequencing data (Chin, Alexander et al. 2013). HGAP is available for use within PacBio's Secondary Analysis Software SMRTPortal. Methodically, the longest subreads of a single SMRT Cell (usually 25x genome coverage, e.g., 25 x 5 Mbp = 125 Mbp) are being chosen to be error-corrected with "shorter" long reads in a process named preassembly. Hereby, a length cut-off is computed automatically separating the "longer" reads (for genome

assembly) and the "shorter" reads (for error-correction). The level of error-correction is being estimated with a per-read accuracy of 99%. Finally, error-corrected long read data is being assembled with Celera Assembler 7.0.

(i) SNV analysis and reconstruction of infecting phages

All short-read sequences were mapped on a high quality closed reference genome of *Vibrio alginolyticus* Strain K01M1 (Wendling et al., 2017) using Bowtie2 (Langmead & Salzberg, 2012). Single nucleotide variation (SNV) analysis was done using the Breseq pipeline as described in Deatherage & Barrick, (Deatherage & Barrick, 2014). Assembly of reads were done using Spades (Bankevich et al., 2012). Whole genome alignments have been calculated using the MAUVE aligner (Darling, Mau, & Perna, 2010). Presence of infecting phage genomes were determined by assembling NGS-reads that did not map on the K01M1 genome in a bowtie2 mapping using Spades. The resulting contigs were annotated based on the review of Mai-Prochnow on filamentous phages (Mai-Prochnow et al., 2015). The genomes of the evolved phages were compared to the infecting phage genomes *Vibrio* phage VALGΦ8 as well as to the genome of the resident prophage *Vibrio* phage VALGΦ6 from the challenged strain K01M1 using BLAST and Easyfig 2.1 (Sullivan, Petty, & Beatson, 2011).

Coverage analysis of phage derived short reads were mapped against the complete ancestral genome of *V. alginolyticus* K01M1 (NCBI accession numbers CP017889.1, CP017890.1) as well as the phage genomes VALGΦ6 and VALGΦ8 using Bowtie2. The resulting coverage data was visualized using Artemis (Version) and compared for differences in coverage. Coverage analysis of Sequel long-reads was performed within the "Base Modification Analysis" within SMRTlink 8 using the same reference as stated

above or additionally including the infecting phage. Coverage data was visualized within SMRTlink.

(j) Statistical analyses

All statistics were performed in the R 3.1.2 statistical environment (Team 2011). For all analysis aimed to compare the two different phage treatments to one another, control populations (i.e., those that evolved without phages) were excluded. When comparing temporal dynamics between phage-treatments, we excluded the starting time-point T0, because these measurements were taken before phages were added to the populations.

Bacteria and phage dynamics

Bacterial and phage densities were analysed over time using a generalized least squares model to control for autocorrelation of residuals over time using the gls function (package nlme) with phage treatment, transfer as categorical variable as well as their interaction as fixed effect.

We considered phages to be prevalent in the population if opaque zones of reduced growth were visible during standard spot assays. Phage prevalence was subsequently quantified by a serial dilution, which were assigned with invers values (i.e., if reduced growth zones were visible up to dilution of 10^{-6} we assigned to it a value of 7, whereas if they were only visible on an undiluted spot, we assigned to it a value of 1, if no zone of reduced growth was visible it was scored as 0). Phage extinction events across phage-treatments were analysed using a log-rank test.

Measuring bacterial resistance

We observed a bimodal histogram on all RBG values with a local minimum at RBG = 0.82 (Figure S1). Thus, we considered an infection as positive if RBG < 0.82. The proportion of resistant clones per population as well as the proportion of clones that tested positive for PCR (targeting the co-evolving phage) were analysed using a generalized linear model with a binomial error distribution using the glm function (package lme4) with phage treatment, transfer and their interaction as fixed effect.

Fitness effects

We determined differences in relative fitness between MSHA-mutants and phage-carrier using a linear model with resistance mechanisms and GFP-label and the interaction thereof as fixed effects. To determine differences in the amount of free phages and in growth rates produced between ancestral strains and evolved strains and between both resistance forms, we used Welch's pairwise *t*-tests with sequential Bonferroni correction. We further performed a Pearson's correlation analysis to determine whether phage production impacted bacterial growth rates.

RESULTS

Bacterial densities

We propagated six replicate populations of *Vibrio alginolyticus* K01M1 in the presence of two closely related filamentous phages, that differed in their virulence: VALGΦ8$_{K04M5}$ (high virulence), VALGΦ8$_{K04M1}$ (low virulence) - or without a phage (control) over 30 serial transfers for ~240 bacterial generations. Phages reduced bacterial densities in both phage-containing treatments by several orders of magnitude compared to control populations (Figure 1a). However, the immediate reduction (measured 24 hours post infection [hpi]) in bacterial density was stronger in populations co-evolving with high virulent phages than with low virulent phages (Figure 1a), confirming that VALGΦ8$_{K04M5}$ is more virulent than VALGΦ8$_{K04M1}$. Over time, however, the densities of bacterial populations co-evolving with high virulent phages recovered three times faster than populations co-evolving with low virulent phages (significant phage:transfer interaction in gls-model: $F_{15,186}$=6.58, p<0.001, Figure 1a).

Phage densities

In both phage containing treatments, phages, that had initially been added at a titre of ~5 ×10^{10} PFU/ml, amplified massively during the first couple of bacterial generations and reached levels of 3.01×10^{12} PFU/ml (VALGΦ8$_{K04M5}$) 24 hpi and 2.83×10^{12} PFU/ml (VALGΦ8$_{K04M1}$) 48 hpi (Figure 1b), before production decreased to levels comparable to phage-free populations. These data suggest that the strong reduction in bacterial densities at the beginning of the experiment (Figure 1a) directly resulted from the production of viral particles (Figure 1b).

We further observed that phage extinction events differed significantly between treatments (log-rank test: $Chisq_1$=4.9, p=0.03). High virulent phages went extinct in five

365 out of six populations after 12 transfers, whereas low virulent phages survived in four
366 out of six populations until transfer 28, before they finally went extinct on transfer 30
367 (Figure S2). To understand the evolutionary drivers behind these different selection
368 dynamics against both phages, we next isolated 24 random clones per population from
369 seven selected transfers and quantified the fraction of phage-resistant clones per
370 population.

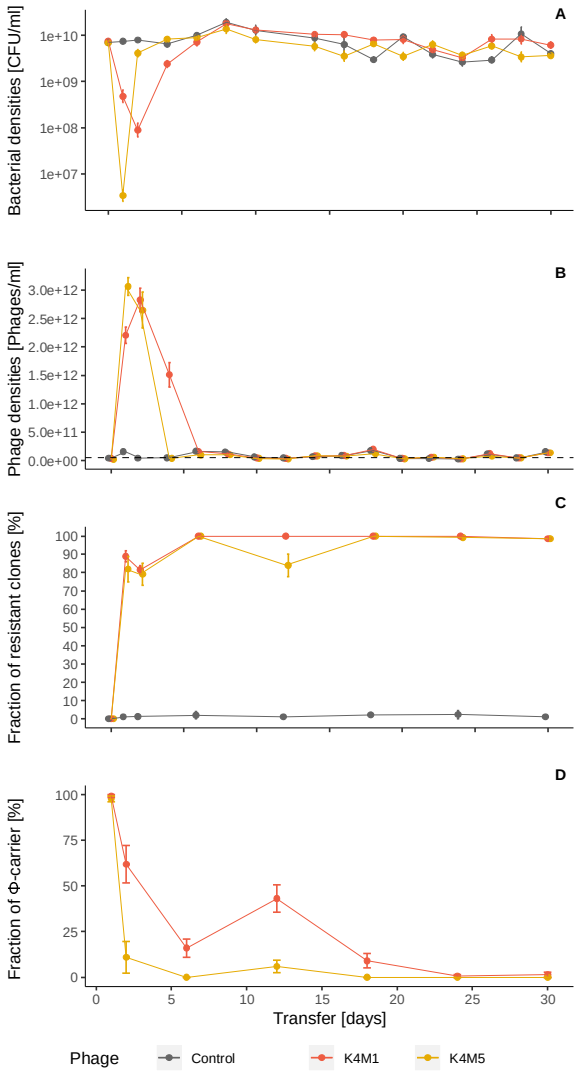

371

372 **Figure 1 Population dynamics over 30 transfers of bacteria-phage co-evolution.** (a) Bacteria in
373 CFU/ml, (b) Phages in PFU/ml, the grey dashed line represents the detection limit for quantifying
374 filamentous phages using spectrophotometry, (c) Fraction of phage-resistant clones (n=24), and (d)
375 Fraction of Φ-carrier within phage-resistant clones. Fractions are based on 24 random clones per replicate
376 population. In all panels, data are represented as mean of six replicate populations per treatments, error
377 bars represent standard errors. Colours correspond to one of three phage-treatments, low virulent
378 VALGΦ8$_{K04M1}$ (red), high virulent VALGΦ8$_{K04M5}$ (yellow), no phage (grey).

Φ-carrier buy time for phage-resistant mutants to rise and sweep through fixation

Different mechanisms can confer resistance to filamentous vibriophages, such as superinfection exclusion, (i.e. when the same phage is already present in the host cell (Wendling, Piecyk et al. 2017)) or surface-receptor modifications, in particular at the mannose-sensitive hemagglutinin (MSHA) type IV pilus, that prevents filamentous vibriophages from entering the host (Jouravleva, McDonald et al. 1998). To determine the underlying genetic basis of the resistance mechanism in the present study, we first selected 24 random clones from each population for a PCR-based analysis to determine presence/ absence of the co-evolving phage. Presence of the co-evolving phage confers resistance through superinfection exclusion. Absence of the co-evolving phage suggests the presence of other resistance mechanisms. This was followed by whole genome sequencing (WGS), for which we randomly selected two clones from each population (one PCR-positive and one PCR-negative clone). WGS analysis confirmed, that clones with a positive PCR result (i.e., Φ-carrier), contained the respective co-evolving phage. Interestingly, in all sequenced PCR-positive clones the co-evolving phage existed exclusively episomal, irrespective of its infection mode in its ancestral host (integrative VALGΦ8$_{K04M5}$ or episomal VALGΦ8$_{K04M1}$). Even though the ancestral K01M1 strain had at least two known integration sites (Supplementary material Figure S3), VALGΦ8$_{K04M5}$ which also exists integrative in several other environmental *Vibrio alginolyticus* isolates (Chibani, Hertel et al. 2020), was not able to integrate into the chromosome of K01M1. Moreover, we observed no genomic changes between ancestral and evolved versions of the two co-infecting phages (VALGΦ8$_{K04M1}$ and VALGΦ8$_{K04M5}$) as well as between the integration sites of the ancestral and evolved

clones. This suggests that the failure to integrate is not a result of genomic changes in the phage nor the integration site that would have prevented phage integration.

Small nucleotide variant (SNV) analysis of the WGS data from all clones that co-evolved with a phage relative to the ancestor revealed no loci with mutations on chromosome 2 and the plasmid pl9064. On chromosome 1 we identified 12 loci with mutations that were not present in clones from the control treatment. Of these 12 loci, three were randomly distributed across PCR-positive and PCR-negative clones while the remaining nine loci were exclusive to PCR-negative clones suggesting a potential role in phage resistance. Of these nine loci, eight had substitutions, duplications, insertions or deletions in four different proteins belonging to the MSHA type IV pilus operon (*mshL, mshE, mshG, K01M1_28150;* Figure 2a/ Table S1). Of these, five caused severe frameshift mutations that presumably have a high impact on the function of this protein. The observed variations occurred in 8/12 PCR-negative clones which suggests strong parallel evolution of phage resistance. Most of the detected mutations fall into genes within the MSHA operon which are highly conserved across *Vibrio* clades (Figure 2b). This suggests, that, similar to other vibrios (Jouravleva, McDonald et al. 1998), the MSHA type IV pilus plays an important role in resistance against the filamentous *Vibrio* phage VALGΦ8. Note, a search of all assembled genomes for CRISPR associated genes as well as for CRISPR array like repetitive sequence patterns did not yield any results. All PCR-negative phage resistant clones are from here onwards referred to as MSHA-mutants.

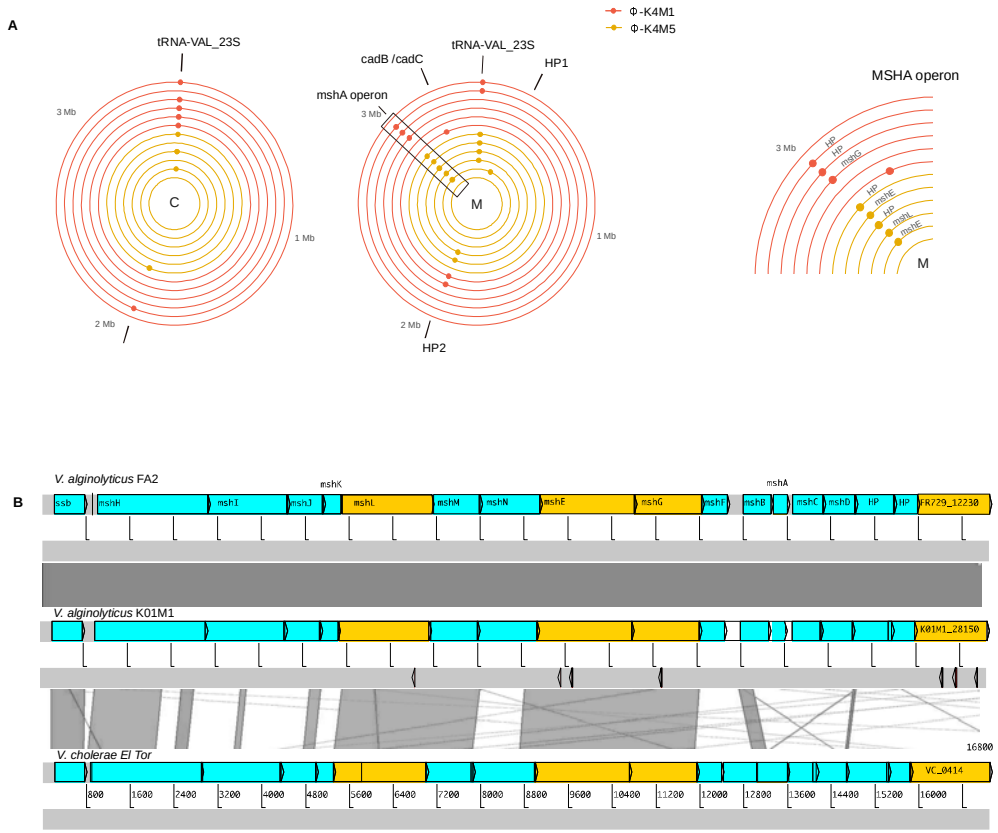

Figure 2 (A) Genetic loci on chromosome 1 under positive selection as indicated by parallel genomic evolution in populations co-evolving with phages: left: Φ-carrier; middle: mutants; right zoom into MSHA-operon region from mutants. Only loci which are not present in control populations are shown. Concentric circles correspond to one clone isolated from either the VALGΦ8$_{K04M5}$ treatments (5 inner circles, yellow) or the VALGΦ8$_{K04M1}$ treatment (six outer circles, red). Each coloured point corresponds to one mutation event on the respective clone. HP corresponds to locus tag K01M1_28150. For more detailed information on the underlying mutation see Table S1.
(B) Structure of the MSHA-operon and comparative genomics comprising MSHA operons from *V. alginolyticus* FA2 (top), *V. alginolyticus* K01M1 (middle), and *V. cholerae* El Tor (bottom). Similarity between regions is indicated by dark grey blocks, genes with detected mutations are marked in orange, detected mutations are marked as arrows below *V. alginolyticus* K01M1.

The proportion of phage-resistant clones per population increased rapidly within the first 24 hours (Figure 1c). This was true for both phage treatments in which we observed almost 100% phage-resistant clones after 24 hours. After 24 hours, Φ-carriers, were the dominating form among the resistant clones (Figure 1d), suggesting that superinfection exclusion is a fast way to acquire phage resistance. However, 48 hours post infection (i.e., on transfer 2) the proportion of Φ-carriers declined, and the MSHA-resistant mutant started to sweep through the populations, suggesting that MSHA-resistant

444 mutants were significantly fitter than Φ-carriers. MSHA-resistant mutants increased
445 significantly faster in populations co-evolving with high virulent, compared to low
446 virulent phages (Figure 1d, significant phage:transfer interaction: $F_{6,60}$=10.18, p<0.001).
447 While Φ-carriers were driven to extinction by MSHA-mutants in all six populations co-
448 evolving with high virulent phages 12 days post infection, Φ-carriers were able to
449 persist, even though at very low frequencies, in five out of six populations co-evolving
450 with low virulent phages until the end of the experiment (i.e., transfer 30). These data
451 suggest that the fitness benefit of MSHA-mutants relative to phage-carriers was higher
452 in populations co-evolving with high virulent phages. This was confirmed in a separate
453 pairwise competition experiment, in which we quantified fitness advantages of MSHA-
454 mutants relative to Φ-carriers (Figure S4). Again, the fitness benefit of MSHA-mutants
455 relative to Φ-carriers was higher when bacteria carried the high virulent phage
456 compared to carriers of the low virulent phage (significant treatment term in linear
457 model with treatment, GFP-label and the interaction thereof as fixed factors: $F_{1,8}$=18.63,
458 p=0.003, Table S2). These results support the dynamics observed in the selection
459 experiment, (i.e., VALGΦ8_{K04M5}-carriers went extinct significantly faster than
460 VALGΦ8_{K04M1}-carriers), confirmed that Φ-carriers can be rapidly outcompeted by
461 MSHA-mutants and demonstrate that the strength of selection is higher in high virulent
462 infections.

463 Given the rapid increase of phage-resistance in the co-evolving populations it is
464 perhaps surprising that the recovery of bacterial populations back to initial densities
465 (i.e., before phages were added to the populations) did not correlate with the absolute
466 number of phage-resistant clones per populations (Pearson's correlation: r=-0.17, t_{78}=-
467 1.55, p=0.13). Moreover, bacterial population densities are negatively correlated with
468 the number of Φ-carriers per population (Pearson's correlation without zero inflation Φ-

K04M1: r=0.69, t_{21}=-4.38, p<0.001, Φ-K04M5: r=0.92, t_7=-6.29, p<0.001; Figure S5). This implies that, even though the majority of the clones in the populations were resistant to the co-evolving phages, bacterial populations were not able to recover as long as the dominating mechanism of phage-resistance was superinfection exclusion. Only when the fraction of Φ-carriers declined, and the fraction of MSHA-mutants increased, bacterial populations started to recover. Accordingly, superinfection exclusion might be a fast way for a bacterial population to gain resistance against filamentous phages. By doing so, Φ-carriers can buy time for resistance mutations to arise and sweep through populations. However, if filamentous phages do not provide a selective benefit, Φ-carriers and ultimately the phage will be lost from the population, once a phage resistant mutant emerges. To further quantify the parameters that influence the increased fitness of MSHA-mutants relative to Φ-carriers, we measured the amount of free phages and the absolute growth rate of selected clones.

Production of free phages is costly

Filamentous phages can produce very high titres in the initial phase of an infection (Lerner and Model 1981), which often results in a strong reduction in bacterial growth and thus high fitness costs. To test whether this observation is true for our system, we quantified differences in phage production and tested if phage production impairs bacterial growth. While Φ-carrier that acquired low virulent phages produced approximately the same number of free phages as in their original host K04M1 (non-significant paired *t*-test: $t_{4.2}$=-1.18, p=0.3, Figure S6a), we observed a significant increase in phage production for high virulent phages once they infected the co-evolving host K01M1 compared to their original host K04M5 (paired *t*-test: t_5=-4.31, p=0.008). Also, VALGΦ8$_{K04M5}$-carriers produced significantly more free phages than

494 VALGΦ8$_{K04M1}$-carriers (paired *t*-test: $t_{5.61}$=-3.36, p=0.017).

495 Direct comparisons of growth rates among evolved clones revealed a significant
496 difference between both resistance forms with Φ-carrier growing on average slower
497 than MSHA-mutants (VALGΦ8$_{K04M5}$: paired *t*-test: $t_{6.61}$=-3.39, p=0.006;
498 VALGΦ8$_{K04M1}$: paired *t*-test: $t_{7.5}$=-3.32, p=0.01, Figure S6b). We further observed that
499 phage production significantly impaired bacterial growth (significant negative
500 correlation between the amount of produced phages and bacterial growth rate Figure 3).
501 This might explain the different dynamics between both phage-treatments in the
502 selection experiment. Accordingly, high virulent phages impose a greater cost to their
503 host than low virulent phages (production of more free phage particles resulted in a
504 stronger reduction of bacterial growth), leading to a stronger selection against bacteria
505 carrying high virulent phages and ultimately a faster extinction. This further explains
506 the earlier stop of the massive initial phage amplification for populations co-evolving
507 with high virulent phages and the faster recovery of the bacterial population to pre-
508 infection densities.

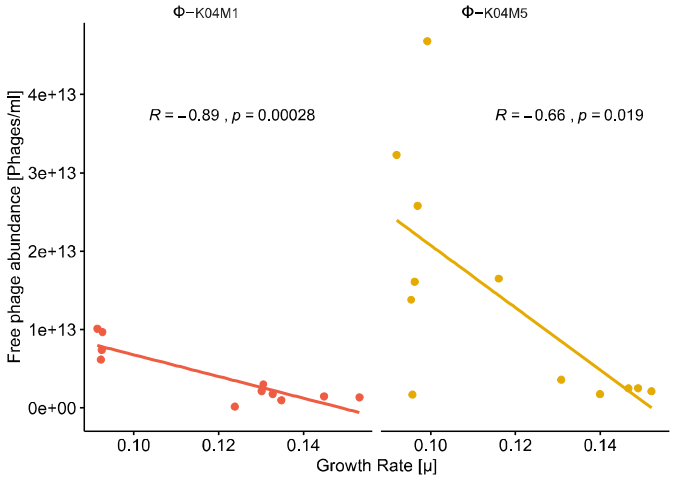

509

510 **Figure 3** Correlation between bacterial growth rate [μ] and production of free phages measured as
511 PFU/ml per clone (left VALGΦ8$_{K04M1}$, right: VALGΦ8$_{K04M5}$).
512

DISCUSSION

We hypothesised that selection for resistance evolution in viral infections will be stronger for high virulent compared to low virulent viral infections. Resistance against filamentous phages can emerge via two ways: (1) super-infection exclusion mediated by the presence of the infecting phage in the bacterial host cell, or (2) molecular resistance evolution, for instance surface-receptor modifications, which prevent phages from entering host cells. Here, we show that upon phage infection, the first way of resistance acquisition was by super-infection exclusion, which occurred at a similar rate in both treatments. However, over time, these phage-carrying clones were rapidly replaced by phage resistant mutants. This replacement happened significantly faster in high virulent compared to low virulent infections, suggesting that selection for molecular resistance evolution is stronger in high virulent infection. Ultimately this faster resistance evolution caused a faster extinction of phages, which were not able to co-evolve in order to overcome evolved host-resistance, and a shorter epidemic.

At least two mutually non-exclusive scenarios can explain why mutants became the dominant form in our experiments: (1) cost of resistance, and (2) stability of resistance. While resistance acquisition is faster via super-infection exclusion than by molecular changes, our data suggest that this process is less stable. That is because in episomal, non-integrative phage infections some bacterial daughter cells will not inherit the infecting phage due to spontaneous segregation-loss, rendering them once again susceptible to subsequent infections. In contrast, molecular resistance evolution is more stable and due to their higher fitness, those resistant clones can rapidly sweep through the population and reach fixation.

The rapid extinction of phages and phage-carriers in our experiment raises the questions, why filamentous phages are omnipresent in nature (Roux, Krupovic et al.

538 2019), including in environmental Vibrio strains closely related to our model strain
539 K01M1 (Chibani, Hertel et al. 2020). In other words, what selects for the presence of
540 filamentous phage-carriers in nature? In some cases filamentous phages can contribute
541 positively to the host's evolutionary fitness (Hay and Lithgow 2019) through lysogenic
542 conversion, i.e., by providing the bacterial host with new phenotypes induced by phage-
543 encoded proteins (Waldor and Mekalanos 1996). In certain environments this may be
544 beneficial enough to outweigh the costs, resulting in a successful chronic infection.
545 Among those, the most prominent example is CTXφ, which carries the genes for the
546 cholera toxin (Waldor and Mekalanos 1996). For the phage from our study, however,
547 we can only speculate, that its presence provides a fitness advantage in the natural
548 environment, which we did not capture in our laboratory experiments. These might
549 include for instance advantages during colonization (Davis and Waldor 2003), or
550 increased stress tolerance (Yu, Chen et al. 2015). The annotation and comparative
551 genomic analyses of VALGΦ8 based on the available information in today's databases,
552 does however not reveal any known-accessory traits that would support this hypothesis
553 (Chibani, Hertel et al. 2020). Answers might come from co-evolution experiments in
554 more natural environments, for instance inside the gut of marine animals. Such results
555 could then be used to predict the chances of establishing a persistent chronic infection
556 which we assume is likely to depend on ecological and evolutionary factors that
557 determine the net-benefit of the phage on its host (Bull, Molineux et al. 1991, Shapiro,
558 Williams et al. 2016, Shapiro and Turner 2018).

559 Ecological benefits of filamentous phages can arise during species interactions, e.g.,
560 by protecting hosts against infection by other phages (superinfection exclusion), by
561 acting as decoys for mammalian immunity (Sweere, Van Belleghem et al. 2019), or
562 from interactions with the abiotic environment e.g., through stress tolerance (Yu, Chen

et al. 2015). Evolutionary benefits include increased mutation supply, and lysogenic conversion (Waldor and Mekalanos 1996). However, filamentous phages can also be costly, for instance thorugh disruption of functional host genes following chromosomal insertion or a fitness loss due to increased transcriptional load, in particular for phages that reproduce at high frequencies. We predict that the net-benefit of a filamentous phage on its host determines the co-evolutionary outcome of both species. If costs associated with phage carriage exceed the benefits, we expect that phages will be quickly lost from the population as we have seen in the present experiment. By contrast, if phages increase their host's fitness we expect successful chronic infections.

Conclusion

Consistent with our hypothesis we could show that selection for resistance evolution is stronger against high virulent compared to low virulent viral infections. Accordingly, high virulent infections will be cleared faster leading to shorter epidemics which will additionally limit the transmission success of high virulent viruses. However, since the virus in our study failed to co-evolve, this system should not be used as a general model to study resistance evolution. Other outcomes in terms of resistance evolution are to be expected, if viruses co-evolve with their hosts. It might be possible that co-evolution of high virulent viruses is constrained as they have much less time to acquire the necessary mutations that would allow them to overcome host resistance. If this holds true, natural selection might favour low virulent variants, that are able to persist longer inside an organism which not only increases their transmission potential but also their time to co-evolve. Future work will focus on the impact of virulence on the evolutionary potential during host-virus co-evolution.

587 **Acknowledgements**: We thank Katja Trübenbach, Veronique Merten, Silke-Mareike
588 Merten and Kim-Sara Wagner for their support in the laboratory.

589

590 **Funding**: This project was funded by two grants from the DFG [WE 5822/ 1-1], [WE
591 5822/ 1-2] within the priority programme SPP1819 given to CCW and OR and a DFG
592 grant within the Cluster of Excellence 80 “The Future Ocean” given to CCW.

593

References

Anderson, R. M. and R. M. May (1982). "Coevolution of hosts and parasites." Parasitology **85 (Pt 2)**: 411-426.

Bull, J. J., I. J. Molineux and W. R. Rice (1991). "Selection of Benevolence in a Host-Parasite System." Evolution **45**(4): 875-882.

Chibani, C. M., R. Hertel, M. Hoppert, H. Liesegang and C. C. Wendling (2020). "Closely Related Vibrio alginolyticus Strains Encode an Identical Repertoire of Caudovirales-Like Regions and Filamentous Phages." Viruses **12**(12).

Chibani, C. M., O. Roth, H. Liesegang and C. C. Wendling (2020). "Genomic variation among closely related Vibrio alginolyticus strains is located on mobile genetic elements." BMC Genomics **21**(1): 354.

Chin, C. S., D. H. Alexander, P. Marks, A. A. Klammer, J. Drake, C. Heiner, A. Clum, A. Copeland, J. Huddleston, E. E. Eichler, S. W. Turner and J. Korlach (2013). "Nonhybrid, finished microbial genome assemblies from long-read SMRT sequencing data." Nat Methods **10**(6): 563-569.

Davis, B. M. and M. K. Waldor (2003). "Filamentous phages linked to virulence of Vibrio cholerae." Curr Opin Microbiol **6**(1): 35-42.

Ebert, D. (1994). "Virulence and Local Adaptation of a Horizontally Transmitted Parasite." Science **265**(5175): 1084-1086.

Fenner, F. and I. D. Marshall (1957). "A comparison of the virulence for European rabbits (Oryctolagus cuniculus) of strains of myxoma virus recovered in the field in Australia, Europe and America." J Hyg (Lond) **55**(2): 149-191.

Goehlich, H., O. Roth and C. C. Wendling (2019). "Filamentous phages reduce bacterial growth in low salinities." R Soc Open Sci **6**(12): 191669.

Harrison, E., D. Guymer, A. J. Spiers, S. Paterson and M. A. Brockhurst (2015). "Parallel Compensatory Evolution Stabilizes Plasmids across the Parasitism-Mutualism Continuum." Current Biology **25**(15): 2034-2039.

Herre, E. A. (1993). "Population structure and the evolution of virulence in nematode parasites of fig wasps." Science **259**(5100): 1442-1445.

Jouravleva, E. A., G. A. McDonald, J. W. Marsh, R. K. Taylor, M. Boesman-Finkelstein and R. A. Finkelstein (1998). "The Vibrio cholerae mannose-sensitive hemagglutinin is the receptor for a filamentous bacteriophage from V. cholerae O139." Infect Immun **66**(6): 2535-2539.

628 Lenski, R. E., M. R. Rose, S. C. Simpson and S. C. Tadler (1991). "Long-Term
629 Experimental Evolution in Escherichia-Coli .1. Adaptation and Divergence during 2,000
630 Generations." American Naturalist **138**(6): 1315-1341.

631 Lerner, T. J. and P. Model (1981). "The "steady state" of coliphage f1: DNA synthesis
632 late in infection." Virology **115**(2): 282-294.

633 Mai-Prochnow, A., J. G. Hui, S. Kjelleberg, J. Rakonjac, D. McDougald and S. A. Rice
634 (2015). "'Big things in small packages: the genetics of filamentous phage and effects on
635 fitness of their host'." FEMS Microbiol Rev.

636 May, R. M. and R. M. Anderson (1983). "Epidemiology and genetics in the coevolution
637 of parasites and hosts." Proc R Soc Lond B Biol Sci **219**(1216): 281-313.

638 Messenger, S. L., I. J. Molineux and J. J. Bull (1999). "Virulence evolution in a virus
639 obeys a trade-off." Proc Biol Sci **266**(1417): 397-404.

640 Poullain, V., S. Gandon, M. A. Brockhurst, A. Buckling and M. E. Hochberg (2008).
641 "The evolution of specificity in evolving and coevolving antagonistic interactions
642 between a bacteria and its phage." Evolution **62**(1): 1-11.

643 Rakonjac, J. (2012). Filamentous Bacteriophages: Biology and Applications eLS. Ltd:
644 Chichester, John Wiley & Sons.

645 Roux, S., M. Krupovic, R. A. Daly, A. L. Borges, S. Nayfach, F. Schulz, A. Sharrar, P.
646 B. Matheus Carnevali, J. F. Cheng, N. N. Ivanova, J. Bondy-Denomy, K. C. Wrighton,
647 T. Woyke, A. Visel, N. C. Kyrpides and E. A. Eloe-Fadrosh (2019). "Cryptic inoviruses
648 revealed as pervasive in bacteria and archaea across Earth's biomes." Nat Microbiol
649 **4**(11): 1895-1906.

650 Shapiro, J. W. and P. E. Turner (2018). "Evolution of mutualism from parasitism in
651 experimental virus populations." Evolution **72**(3): 707-712.

652 Shapiro, J. W., E. S. C. P. Williams and P. E. Turner (2016). "Evolution of parasitism
653 and mutualism between filamentous phage M13 and Escherichia coli." Peerj **4**.

654 Sweere, J. M., J. D. Van Belleghem, H. Ishak, M. S. Bach, M. Popescu, V. Sunkari, G.
655 Kaber, R. Manasherob, G. A. Suh, X. Cao, C. R. de Vries, D. N. Lam, P. L. Marshall,
656 M. Birukova, E. Katznelson, D. V. Lazzareschi, S. Balaji, S. G. Keswani, T. R. Hawn,
657 P. R. Secor and P. L. Bollyky (2019). "Bacteriophage trigger antiviral immunity and
658 prevent clearance of bacterial infection." Science **363**(6434): 1416-+.

659 Team, R. D. C. (2011). " R: A language and environment for statistical computing. R
660 Foundation for Statistical Computing." Vienna, Austria. ISBN 3-900051-07-0, URL
661 http://www.R-project.org/. .

662 Turner, P. E., V. S. Cooper and R. E. Lenski (1998). "Tradeoff between Horizontal and
663 Vertical Modes of Transmission in Bacterial Plasmids." Evolution **52**(2): 315-329.

664 Waldor, M. K. and J. J. Mekalanos (1996). "Lysogenic conversion by a filamentous
665 phage encoding cholera toxin." Science **272**(5270): 1910-1914.

666 Weiss, S. R. and J. L. Leibowitz (2011). "Chapter 4 - Coronavirus Pathogenesis."
667 Advances in Virus Research **81**: 85-164.

668 Wendling, C. C., H. Goehlich and O. Roth (2018). "The structure of temperate phage-
669 bacteria infection networks changes with the phylogenetic distance of the host bacteria."
670 Biol Lett **14**(11).

671 Wendling, C. C., A. Piecyk, D. Refardt, C. Chibani, R. Hertel, H. Liesegang, B. Bunk,
672 J. Overmann and O. Roth (2017). "Tripartite species interaction: eukaryotic hosts suffer
673 more from phage susceptible than from phage resistant bacteria." BMC Evol Biol
674 **17**(98).

675 Yu, Z. C., X. L. Chen, Q. T. Shen, D. L. Zhao, B. L. Tang, H. N. Su, Z. Y. Wu, Q. L.
676 Qin, B. B. Xie, X. Y. Zhang, Y. Yu, B. C. Zhou, B. Chen and Y. Z. Zhang (2015).
677 "Filamentous phages prevalent in Pseudoalteromonas spp. confer properties
678 advantageous to host survival in Arctic sea ice." ISME J **9**(4): 871-881.
679